

## Oxide ion polarizability, optical basicity, and metallization criterion of GO-coated Nd<sub>2</sub>O<sub>3</sub> (NPs) - TeO<sub>2</sub> glass for linear optical fibre

H. R. Shaari<sup>a</sup>, M. N. Azlan<sup>a,\*</sup>, Y. Azlina, N. M. Al-Hada<sup>b</sup>, S. A. Umar<sup>c</sup>,  
B. K. Kenzhaliyev<sup>d</sup>, M. H. M. Zaid<sup>e</sup>, R. Hisam<sup>f</sup>, N. N. Yusof<sup>g</sup>

<sup>a</sup>*Physics Department, Faculty of Science and Mathematics, University Pendidikan Sultan Idris, 35900 Tanjong Malim, Perak, Malaysia;*

<sup>b</sup>*Shandong Key Laboratory of Biophysics, Institute of Biophysics, Dezhou University, Dezhou 253023, China*

<sup>c</sup>*Department of Physics, Faculty of Science, Federal University Lafia, Lafia, Nasarawa State, Nigeria*

<sup>d</sup>*Institute of Metallurgy and Ore Beneficiation, Satbayev University, Almaty, Kazakhstan;*

<sup>e</sup>*Department of Physics, Faculty of Science, Universiti Putra Malaysia, 43400, Serdang, Selangor, Malaysia;*

<sup>f</sup>*Faculty of Applied Sciences, Universiti Teknologi MARA, 40450 Shah Alam, Selangor, Malaysia;*

<sup>g</sup>*School of Physics, Universiti Sains Malaysia, 11800 USM, Penang, Malaysia*

The versatility of graphene oxide (GO) as coating materials on the glass surface is a new revolution in the advanced glass era. In this work, GO liquid solution was prepared by using electrochemical exfoliation in an electrolyte solution assisted by different surfactants. Meanwhile, a glass series was prepared by using the conventional melt-quenched technique. A low-cost and simple spray deposition technique was used to deposit the GO on the glass sample. The obtained glass series was denoted as GO coated TNd (NPs), meanwhile, the uncoated glass was labelled as uncoated TNd (NPs). The linear optical properties of GO coated TNd (NPs) glass series was determined using UV-Vis spectrophotometer and utilizing the Lorentz-Lorentz equation to determine the value of polarizability. X-ray diffraction spectra revealed the amorphous structural characteristics of the glass series. The SEM morphological image revealed the variation of GO distribution on the glass surface due to the agglomeration and inhomogeneity of GO distribution on the glass surface. The homogeneity of GO distribution on the glass surface is negligible in this work as we focus solely on the effect of GO on glass properties. According to the observations, the value of GO-coated TNd (NPs) is in the range 3.4531-3.8549 Å and uncoated TNd (NPs) is in the range 2.709- 2.774 Å. Meanwhile, the optical basicity value ranges from 1.220 to 1.262. These results demonstrate that the polarizability of oxide ions and optical basicity values of the GO coated TNd (NPs) glass series was higher than the uncoated TNd (NPs) glass. The metallization criterion for the GO-coated TNd (NPs) glass system is in the range of  $0.3 < M < 0.4$ . Based on these results, the obtained glasses are promising in linear optical glass fibre.

(Received May 17, 2022; Accepted August 30, 2022)

**Keywords:** Graphene oxide, Neodymium-doped, Tellurite, Glasses coating, Optical basicity, Metallization criterion

### 1. Introduction

The discovery and availability of nanomaterials such as graphene oxide (GO) have exceptional mechanical, electrical, thermal, optical, and physical characteristics [1]. The excellent properties of GO have been attracted the interest of many applications [2], [3] such as optoelectronics, supercapacitors, energy storage devices such as GO-based lithium rechargeable

---

\* Corresponding author: azlanmn@fsm.ups.edu.my  
<https://doi.org/10.15251/CL.2022.198.565>

batteries, sensor (biosensor) solar cells, catalysts, and photocatalysts [2]–[5]. GO is a hexagonal carbon structure composed of sp<sup>2</sup> and sp<sup>3</sup> hybridised carbon atoms, hydroxyl and epoxy functional groups in the basal plane, and a carboxyl group on the edges [6].

Neodymium-doped phosphate laser glass has been employed in a variety of commercial applications. However, due of the lack of durability, tellurite-based glass is used in laser host materials [7]. Glass materials with higher optical efficiency and refractive index [8] are desirable in laser application as it corresponds to higher absorption and emission cross-section. The solubility and compatibility of neodymium oxide with tellurite glass is really useful for the laser glass. Rare-earth may produce upconversion emission by excitation of two or more near-infrared photons. Because of the 4f-4f orbital interactions surrounding by host materials, the specialities of neodymium in glass may create strong spectral and emission lines. [9, 10].

The inclusion of GO as a coating material on the glass surface of rare-earth-doped tellurite-based glasses has been studied a lot in the last few years. [4], [11], [12]. Azlina et al. discovered that the presence of oxygen-containing functional groups in GO layers improved the optical characteristics of GO coated on rare-earth-doped tellurite glass surfaces for optical fibre. [12]. The combination of graphene oxide with tellurite glass is an excellent strategy for improving the optical characteristics of the tellurite glass network system, since GO is the best choice for producing high-quality glass coatings and would be highly beneficial for fibre optics applications [4]. Utilizing GO as a coating materials on glass surface has increased significantly the refractive index above  $n > 2.0$ . Therefore, these materials have high optical capabilities in fiber optic laser technology [11] and excellent to be used as fiber cores in optical fibers [4].

In this work, we investigate the role of the GO on the oxide ion polarizability, optical basicity, and metallization criterion of neodymium NPs doped tellurite glass system which has never been done before. Thus, the application of nanomaterials in new tellurite glass will provide a higher capability to develop more efficient fiber laser technology and nonlinear optical applications.

## 2. Experimental method

### 2.1. Glass preparation

Using a low-cost melt-quenched process, a series of glass systems with the chemical composition  $(0.47(1-y))\text{TeO}_2 + (0.2(1-y))\text{B}_2\text{O}_3 + (0.29(1-y))\text{ZnO} + (y)\text{Nd}_2\text{O}_3$  (nanoparticles) with  $y = 0.01, 0.02, 0.03, 0.04$  and  $0.05$  were prepared. The raw materials for all compounds were obtained from manufacture as follows, tellurite oxide ( $\text{TeO}_2$ ), (99.99% metals basis), zinc oxide ( $\text{ZnO}$ ), (99.99%, metals basis), boron oxide  $\text{B}_2\text{O}_3$ , (98.5%, metals basis) neodymium oxide (NPs),  $\text{Nd}_2\text{O}_3$  (99.9 %, 20-30nm Nanostructure and Amorphous Materials, Inc.).

Firsly, all the chemical oxides were weighed using a high precision digital weighing scale with  $\pm 0.0001$  g accuracy based on the computation from the chemical compositions of the glass. To obtain a homogenous mixture, the chemical mixture was stirred for 30 minutes using a macro spatula. The alumina crucible mixes were then placed in an electric furnace and warmed at  $400\text{ }^\circ\text{C}$  for 1 hour to eliminate the moisture content. The temperature of the furnace was increased to  $900\text{ }^\circ\text{C}$  after the pre-heating procedure, and the heating process takes 2 hours. The cylindrical stainless steel mould was annealed in an oven at  $300\text{ }^\circ\text{C}$  for 1 hour. After 2 hours, the molten liquid was immediately quenched into a  $400\text{ }^\circ\text{C}$  pre-heated cylindrical stainless steel split mould.

The sample was immediately moved to an annealing procedure that was maintained at  $400\text{ }^\circ\text{C}$  for one hour before the furnace was switched off. The glass sample was made after the annealing procedure. After the annealing process, the glass sample was formed. The glass samples were polished using silicon carbide paper to achieve a flat and smooth glass surface for glass characterisation.

### 2.2. Synthesis of GO and spray coating technique

As illustrated in Figure 1, graphene oxide (GO) was synthesised using an electrochemical exfoliation technique with an ionic  $0.1\text{ mol SDS}$  surfactant as an electrolyte solution, which intercalated graphite rods into a single sheet [13]. The synthesis of GO was discussed in our

previous works [11]. The resulting GO solution was coated on the glass surface using the spray coating procedure depicted in Figure 2.

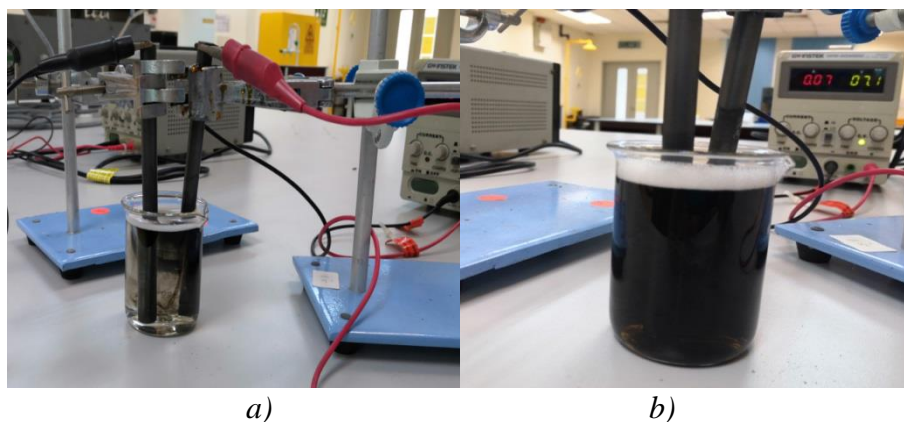


Fig. 1. (a) Assemble the graphite rods as electrolysis process to synthesis the GO using electrochemical exfoliation method. The graphite rods were partially immersed in a prepared 0.1 M SDS surfactant electrolyte and connected to a DC power supply at 7.0 V current. (b) 0.1M SDS-GO dispersion after 24 hours.

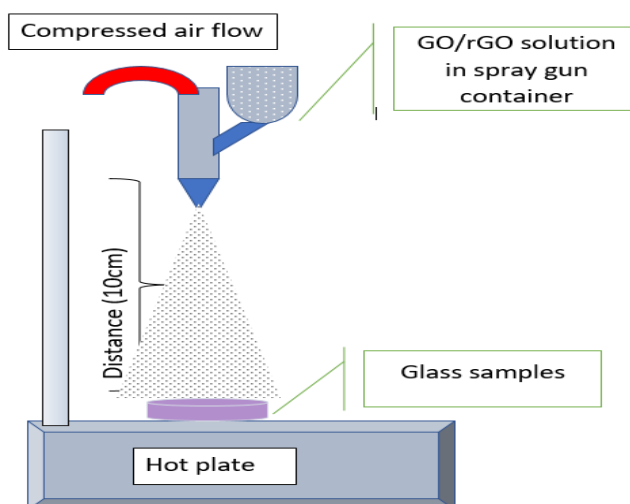


Fig. 2. Spray coating method on glass sample [11].

### 2.3. Characterization of the samples

Figure 3 shows pictures of the glass samples, and their structural properties were assessed using the X-ray Diffraction PANanalytical's EMPYREAN diffractometer. At room temperature, the diffraction patterns were recorded in the theta range  $10^\circ < 2\theta < 80^\circ$  with a wavelength of  $\lambda = 1.54060 \text{ \AA}$  Cu-K $\alpha$  at room temperature. The transmission band of each element in the glass systems was determined using an FTIR NEXUS Thermo 69000 Nicolet instrument. The spectra were collected in the 400-4000  $\text{cm}^{-1}$  region. The surface morphology of graphene oxide on the glass surface was studied using the HITACHI model SU 8020 Field Scanning Electron Microscopy equipment. The optical characteristics of the GO coated TNd (NPs) glasses were measured at room temperature using a UV-Vis-NIR Spectrometer (PerkinElmer Model: Lambda 950) in the range 200–3000 nm of wavelength.



Fig. 3. A series of glass samples after the spray-coating method.

### 3. Result and discussion

#### 3.1. X-Ray Diffraction

X-ray diffraction analysis is a non-destructive method to define the existence of the crystalline phase in the material [14]. Figure 4 illustrated the diffraction pattern of the GO coated TNd (NPs) glass samples at  $2\theta$  angles in the range  $20^\circ$  to  $80^\circ$  at room temperature. A broad hump with an absent sharp peak was observed between  $20^\circ$  to  $35^\circ$ , confirming that the glass samples are entirely amorphous following glass formation [7] and non-existence of a crystalline phase [15].

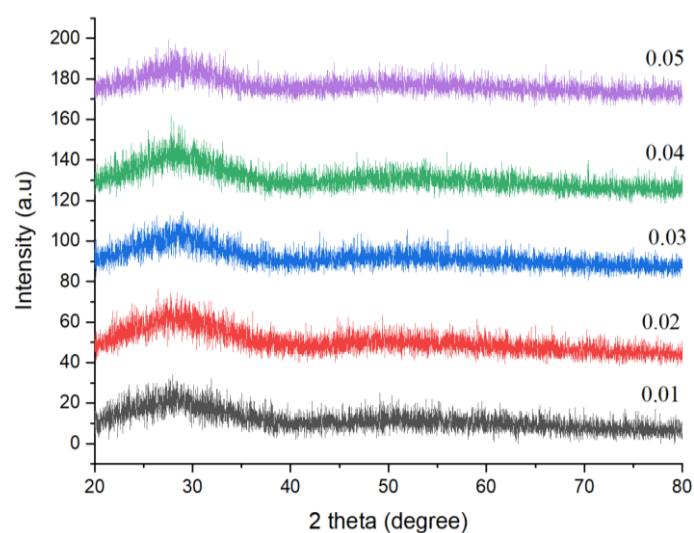


Fig. 4. XRD diffraction pattern of GO coated TNd (Nps) glasses at various concentrations of neodymium molar ratio.

#### 3.2. Scanning Electron Microscopy (SEM) analysis

SEM analysis was conducted to confirm the existence of the GO layer on the glass surface and analyze the distribution of GO. Figure 5 presents the SEM image of the GO coated TNd (NPs) glasses. Thick aggregation and uniformity of GO were seen at a certain area of the glass surface. Inhomogeneous of the GO distribution is due to the the fast exfoliation process and the type of surfactant in electrolyte during GO synthesis [16]. A different concentration of surfactant

affected the agglomeration of GO on the glass samples [12]. The presence of the higher oxygen functional group is due to dispersed of GO sheet assisted SDS surfactant in the water-based system which extend the oxidation process. Based on the exfoliation process, various oxygen is attached to the GO structure [13] According to Kazi et al, GO structure is more agglomerate at the highest defect on basal structure [17]. As a consequence, inhomogeneous structure distribution are formed on glass surface as shown in SEM image at 10 000 magnification.

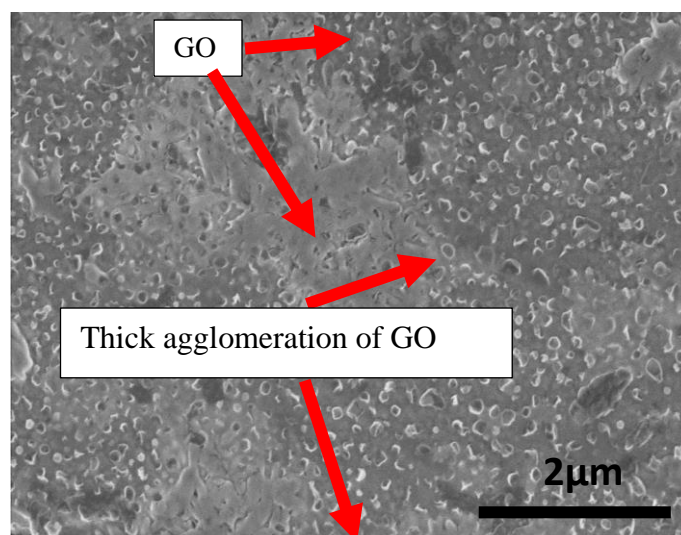


Fig. 5 FESEM micrographs of GO coated TNd (NPs) glass surface at magnification  $\times 10\,000$  magnification.

### 3.3. Absorption spectra analysis

The optical absorption spectra of GO coated TNd (NPs) glasses were presented in Figure 6. XRD analysis revealed that the absorption spectra edges in glass samples are not strongly defined, indicating a non-crystalline/amorphous structure [18]–[20]. There are several peaks that emerge from the ground state ( $^4I_{9/2}$ ) to the excited state. The properties of neodymium ions in the present glass matrix are indicated by these absorption bands. Transitions from from  $^2P_{1/2}$ ,  $^4G_{5/2} + ^2D_{3/2} + ^2K_{15/2}$ , ( $^4G_{9/2}$ ), ( $^2K_{13/2} + ^4G_{7/2}$ ), ( $^2G_{7/2} + ^4G_{7/2}$ ), ( $^2H_{11/2}$ ), ( $^4F_{9/2}$ ), ( $^4S_{3/2} + ^4F_{7/2}$ ), ( $^4F_{5/2} + ^2H_{9/2}$ ), and ( $^4F_{3/2}$ ) are observed around wavelengths of 432, 479, 515, 528, 595, 630, 683, 756, 800 nm respectively [21]–[23]. Because of the f-f interaction of  $Nd^{3+}$  ions, the absorption spectra have numerous in-homogeneously widened bands. Furthermore, the intensity of the absorption band shows an increasing trend due to the increasing concentration of neodymium NPs [10].

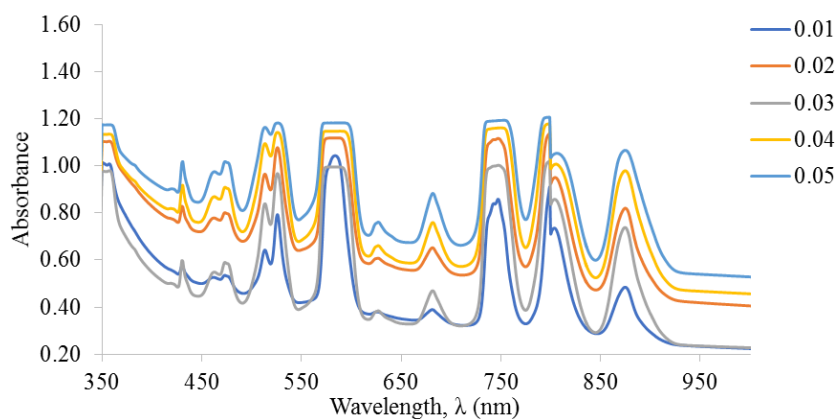


Fig. 6. UV-Vis absorption spectra of GO coated TNd (NPs) glasses.

### 3.4. Energy band gap analysis

Optical absorption analysis is a valuable method for determining the energy band gap of non-crystalline materials. [24]. The indirect optical band gap was calculated from absorption spectra data by using Mott and Davis expression as follows [21].

$$\alpha(\omega) = \frac{\beta(\hbar\omega - E_{opt})^n}{\hbar\omega} \quad (1)$$

where  $\beta$  is a constant that must be zero,  $\hbar\omega$  is the incident photon energy, and  $n$  is the index number that determines the nature of the interband electronic transition. The absorption  $n = 1/2$  denotes an indirect transition that is allowed.

Figures 7 depicts the Tauc's plot of  $(\alpha\hbar\omega)^{1/2}$  for the GO coated TNd (NPs) indirect allowed transitions. Table 1 shows the results of extrapolating the curves to estimate the optical band gap,  $E_{opt}$ , of the glass series. Between 2.665 and 2.405 eV, the optical bandgap value of GO coated TNd (NPs) decreases. At 0.03 molar fraction, the value of indirect band gap is shown increased which is due to the influence inhomogeneous of GO distribution on the glass surface as confirmed in SEM analysis. Furthermore, the observed trend is the result of the formation of oxygen functional groups in GO layers during oxidation. The oxidation process is the main reason for the existence of high oxygen functional groups with localised  $\Pi$  electrons [25]. Aside from that, the GO optical band gap is primarily influenced by the  $\Pi$  and  $\Pi^*$  states [26]. The presence of localised finite-sized molecular  $sp^2$  clusters in the  $sp^3$  matrix will result in  $\pi$ -electrons confinement in the GO. [11]

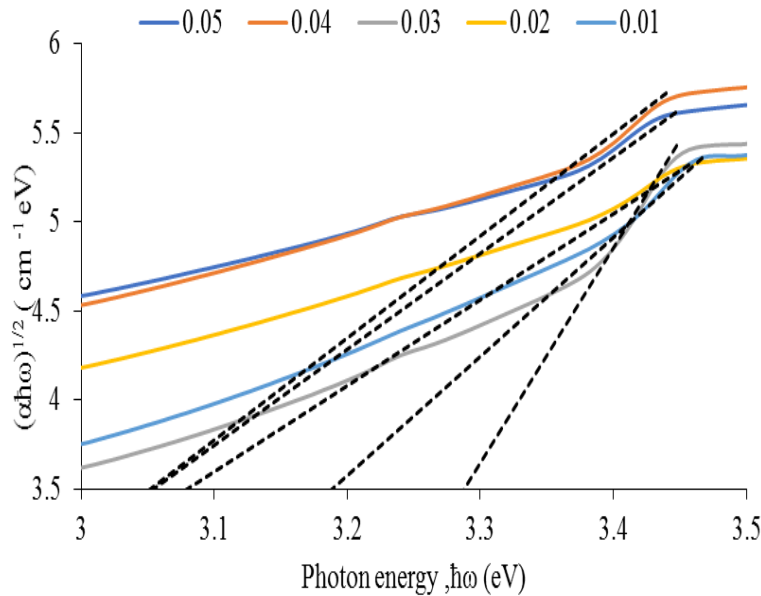


Fig. 7. Indirect band gap  $(\alpha\hbar\omega)^{1/2}$  versus photon energy,  $\hbar\omega$  (eV) for GO coated TNd (NPs) glasses.

Table 1. Indirect optical band gap ( $E_{opt}$ ), GO coated TNd (NPs).

Nd (NPs) molar fraction, x	Indirect band gap, eV
0.01	2.665
0.02	2.355
0.03	2.998
0.04	2.442
0.05	2.405

### 3.5. Oxide ion polarizability

The computation of the polarizability of oxide ions  $\alpha_{o^{2-}}$  is originally from the Dimitrov and Sakka equation which used energy band gap for simple oxide [27]. The polarizability of oxide ions can be obtained by following relationship between  $\sqrt{E_g}$  and  $1 - \frac{R_m}{V_m}$  and was described by Duffy and Ingram [28] for a large number of simple oxides from the following expression

$$E_g = 20 \left(1 - \frac{R_m}{V_m}\right)^2 \quad (2)$$

$$\alpha_{o^{2-}}(E_g) = \left[ \frac{V_m}{2.52} \left(1 - \sqrt{\frac{E_g}{20}}\right) \sum \alpha_i \right] (N_{o^{2-}})^{-1} \quad (3)$$

where  $\alpha_{o^{2-}}(E_g)$  represent energy band gap based polarizability of oxide ions,  $\sum \alpha_i$  represent molar cation polarizability and  $N_{o^{2-}}$  denotes the number of oxide ions in the chemical formula. The molar cation polarizability of  $Te^{4+}$ ,  $Zn^{3+}$ ,  $B^+$  and  $Nd^{3+}$  ions are  $\alpha_{Te} = 1.595 \text{ \AA}^3$ ,  $\alpha_{zn} = 0.283 \text{ \AA}^3$ ,  $\alpha_B = 0.002 \text{ \AA}^3$ ,  $\alpha_{Nd} = 2.546 \text{ \AA}^3$ . The calculated value of polarizability of oxide ions of GO coated TNd (NPs) and uncoated TNd (NPs) are plotted in Figure 8 and tabulated in Table 2 respectively.

The lowest value of polarizability of oxide ions is found at 0.03 mol fraction. This trend may be due to the role of zinc oxide in the glass system. Azlina et al, [10] stated that zinc oxide has a dual nature and serves as a modifier or former glass. According to Dimitrov and Komatsu, zinc oxide,  $Zn^{4+}$ , has a large cationic charge with a strong unit field strength [29]. As a result, zinc oxide may behave like a former glass at 0.03 mol fraction resulting in a decrease in oxide ion polarizability [10]. The inclusions of small particles in tellurite network may contributes to the structural changes in the glass network that influence the oxide ion polarizability [30]. However, the type of link between oxygen and graphene gives a significant effect in the polarizability of oxide ions.

The coating of GO on the glass surface consists of oxygen functional groups on the present glasses system which influence the value of oxide ion polarizability. The obtained data revealed that the GO coated TNd (NPs) value are high and in the range 3.4531- 3.8549 $\text{\AA}$ , meanwhile, the uncoated TNd (NPs) glass is low and in the range 2.709- 2.774 $\text{\AA}$  [10]. It can be assumed from this pattern that the link between oxygen and graphene is stronger than the bond between oxygen and the glass network. As a result, it is doubtful that the oxygens in graphene layers are more polarizable. However, the non-linear trending in the plotted graph is due to the lack of homogeneity of GO distribution on the glass surface [4].

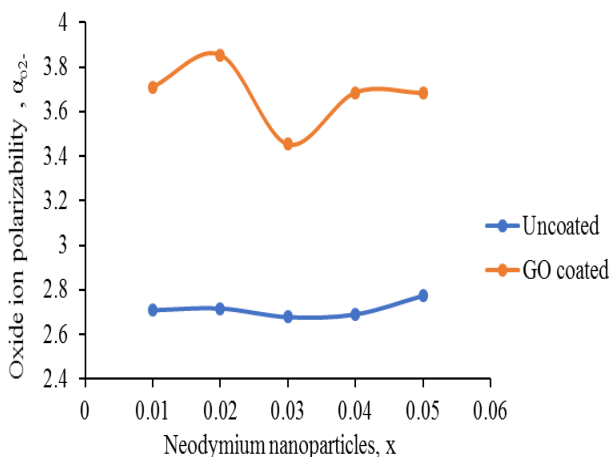


Fig. 8. Oxide ion polarizability versus molar fraction of GO coated TNd (NPs) and TNd (NPs) glasses.

Table 2. Oxide ion polarizability of GO coated TNd (NPs) and TNd (NPs) glasses.

Molar fraction, x	Oxide ion polarizability, $\alpha_{o2}$ GO coated TNd (NPs) glasses	Oxide ion polarizability, $\alpha_{o2}$ uncoated TNd (Nps) glasses
0.01	3.711	2.709 [10]
0.02	3.854	2.717 [10]
0.03	3.453	2.678 [10]
0.04	3.686	2.690 [10]
0.05	3.684	2.774 [10]

### 3.6. Optical basicity

The ability of the oxide ion to give electrons (negative charge) to the surrounding cation in the glass network is referred to as optical basicity. The theoretical bulk optical basicity multi component glasses can be determined from Duffy and Ingram equation as reported by [21], [29].

$$\Lambda_{th} = x_1 \Lambda_1 + x_2 \Lambda_2 + \dots x_n \Lambda_n \quad (4)$$

where  $X_1, X_2 \dots X_n$  is are equal fractions based on the quantity of oxygen contributed by each oxide to the overall glass stoichiometry, and  $\Lambda_1, \Lambda_2 + \Lambda_n$  are basicities that correspond to the individual oxides in the glass system. The relationship between polarizability of oxide ions and optical basicity proposed by Duff [30], [31] can be used to predict optical basicity.

$$\Lambda = 1.67 \left( 1 - \frac{1}{\alpha_{o2-}} \right) \quad (5)$$

The obtained data of optical basicity for GO coated TNd (NPs) glasses are plotted in Figure 9 and tabulated in Table 3. The values of optical basicity vary in the range of 1.220 to 1.262 for the present glass system. Figure 9 depicts the non-linear optical basicity distribution, which exhibits an increasing trend in optical basicity from 0.03 to 0.05 mole fraction. This difference can be attributed to the present glasses increased oxide ion polarizability as compared to uncoated TNd (NPs) glasses.

However, the reduction value of optical basicity from 0.02 to 0.03 mole fraction is may be due to the agglomeration of graphene oxide on the glass surface, where the basal structure of aromatic carbon rings promotes a strong tendency for hydrophobic contacts between particles [17]. Moreover, the increasing trend of optical basicity may be due to ZnO which has a higher basicity value (0.82) than borate oxide (1.75) [32]. According to Azlan et al., [33], an increase in optical basicity indicates an increase in the ability of oxide ions to donate electrons to the surrounding cation. Additionally, as the polarizability of oxide ions increases, the optical basicity of the glass system increases [30]. As a result, a rise in optical basicity in the current glasses suggests an improvement in ionic characteristics.



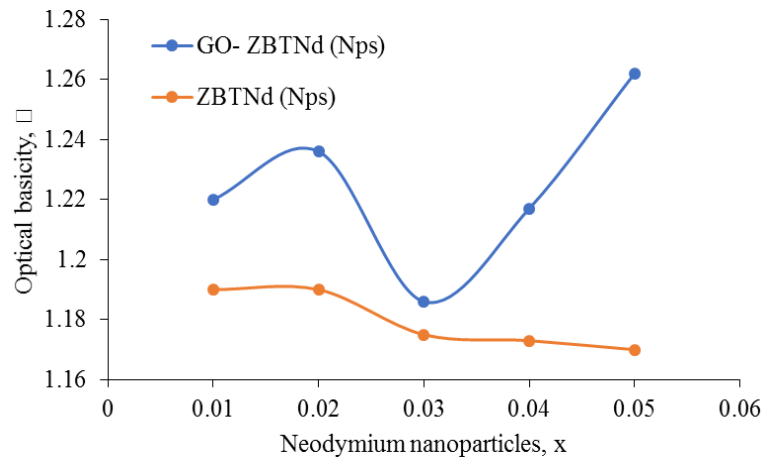


Fig. 9. Optical basicity versus neodymium NPs molar fraction of GO coated TNd (NPs) and uncoated TNd (NPs) glasses.

Table 3. Optical basicity of GO coated neodymium NPs doped ZBT glasses.

Neodymium Molar Fraction	Optical basicity of GO coated TNd (NPs) glasses	Optical basicity of TNd (NPs) glasses
0.01	1.220	1.190 [10]
0.02	1.236	1.190 [10]
0.03	1.186	1.175 [10]
0.04	1.217	1.173 [10]
0.05	1.262	1.170 [10]

### 3.7. Metallization criterion

Calculating the metallization criterion value can be used to make predictions about metallic and non-metallic processes in glass systems. According to Dimtrov and Sakka [34], that two requirements represent the glass system's nature: a metallization criterion value less than one shows that the glass samples are metalizing, and a metallization criterion value near one indicates that the manufactured glass is an insulator [30]. The equation shown below [29], [35] can be used to compute the metallization criterion M value.

$$M = 1 - \frac{n^2 - 1}{n^2 + 2} = \sqrt{\frac{E_g}{20}} \quad (6)$$

Table 4 shows the computed values of the metallization criteria for GO TNd (Nps) glasses as well as the uncoated TNd (Nps) glasses. The metallization criterion for the present glass exhibit decreasing trend in the range 0.387 to 0.343, meanwhile, for uncoated TNd (Nps) glasses lies in the range 0.517 to 0.485 [10] respectively as shown in Figure 10. The diminishing trend in the metallization criteria for GO-coated TNd (NPs) glasses can be attributed to the effect of GO layers, which contain a high concentration of oxygenated functional groups, hence improving the optical performance of glass materials. The decreasing values of optical bandgap and the rise in the refractive index affected the metallization criterion value of the GO coated TNd (NPs) glasses [36]. From the literature, the obtained values show that the GO coated TNd (NPs) glass system glasses have a great deal of promise for use in laser and non-linear optical applications [30], [37], [38].

Table 4. Metallization criterion of GO- ZBT glasses, and metallization criterion uncoated TNd (Nps), [10].

Neodymium Molar Fraction	Metallization criterion, GO coated TNd (NPs) (present study )	Metallization criterion uncoated TNd (NPs),
0.01	0.365	0.517 [10]
0.02	0.343	0.514 [10]
0.03	0.387	0.506 [10]
0.04	0.349	0.501 [10]
0.05	0.347	0.485 [10]

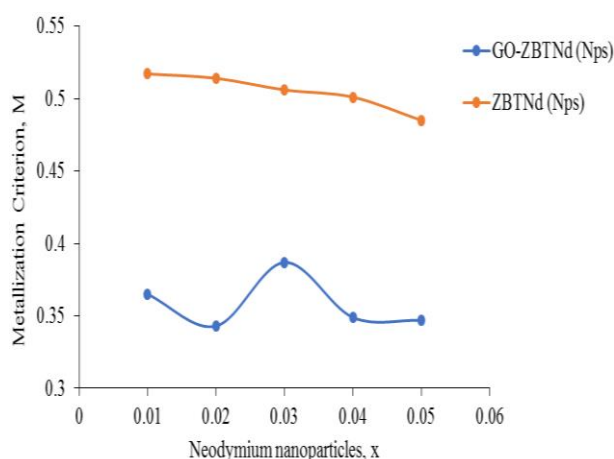


Fig. 10. Metallization criterion versus neodymium NPs molar fraction of GO coated TNd (NPs) and uncoated TNd (NPs) glasses

#### 4. Conclusions

As conclusion, polarizability of oxide ion, optical basicity and metallization criterion based on energy band gap have been calculated theoretically for the quaternary  $(0.47(1-y))\text{TeO}_2 + (0.2(1-y))\text{B}_2\text{O}_3 + (0.29(1-y))\text{ZnO} + (y)\text{Nd}_2\text{O}_3$  (nanoparticles) which fabricated by using the conventional melt-quenching method. The findings of this research are as follows:

Deposited graphene oxide on glass surface consisting of the presence of oxygen functional groups on the present glasses system influence the value of oxide ion polarizability. The observed shown that the GO coated TNd (NPs) value higher in the range  $3.4531 - 3.8549 \text{ \AA}$  than uncoated TNd (NPs) in the range  $2.709 - 2.774 \text{ \AA}$ .

The increasing the polarizability of oxide ions give the increasing trend of optical basicity also due to the presence of the GO. The higher optical basicity gives the ability of oxide ions donor electron to surrounding cation. As a result, a rise in optical basicity in the current glasses suggests an improvement in ionic characteristics. Metallization criterion values of the GO-TNd (NPs) glass system in the range  $0.3 < M < 0.4$  show that these glasses have a great deal of promise for use in laser and non-linear optical applications.

#### Acknowledgements

The authors would like to thank to Skim Geran Penyelidikan Fundamental (FRGS) Fasa 1/2018 (Grant code: 2019-0006-102-02) for grant support.

## References

- [1] P. Bondavalli, D. Pribat., P. Legagneux., M.B, Martin., L, Hamidouche., L, Qassym., G, Feugnet., A.F, Trompeta, C.A, Charitidis. Deposition of graphene and related nanomaterials by dynamic spray-gun method: A new route to implement nanomaterials in real applications, *JPhys Materials*. 2(3), 032002 (2019)  
<https://doi.org/10.1088/2515-7639/ab1795>
- [2] M. K Kavitha, and M. Jaiswal. Graphene : A review of optical properties and photonic applications, *Asian Journal of Physics*. 25(7), 809-831 (2016)
- [3] R. M. Gerosa, F. G. Suarez, P. G. Vianna, S. H. Domingues, and C. J. S. de Matos, One-step deposition and in-situ reduction of graphene oxide in photonic crystal fiber for all-fiber laser mode locking, *Opt. Laser Technol.* 121, 105838 (2020).  
<https://doi.org/10.1016/j.optlastec.2019.105838>
- [4] Y. Azlina, M.N. Azlan, S. S. Hajer, M. K. Halimah, A.B. Suriani, S.A. Umar, R. Hisam, M. H. M. Zaid, S. M. Iskandar, B.K. Kenzhaliyev, A.V. Nitsenko, N. N. Yusof, and B. Imed. Graphene oxide deposition on neodymium doped zinc borotellurite glass surface: Optical and polarizability study for future fiber optics, *Opt. Mater.* 117, 111138 (2021)  
<https://doi.org/10.1016/j.optmat.2021.111138>
- [5] A. T. Dideikin and A. Y. Vul', Graphene Oxide and Derivatives: The Place in Graphene Family, *Front. Phys.* 6, 149 (2019)  
<https://doi.org/10.3389/fphy.2018.00149>
- [6] N. U. Kiran, S. Dey, B. P. Singh, and L. Besra, Graphene coating on copper by electrophoretic deposition for corrosion prevention, *Coatings*. 7, 214 (2017)  
<https://doi.org/10.3390/coatings7120214>
- [7] N. A. M. Jan, M. R. Sahar, S. Sulhadi, R. El-Mallawany. Thermal, structural and magnetic properties of TeO<sub>2</sub>-MgO-Na<sub>2</sub>O-Nd<sub>2</sub>O<sub>3</sub> glass system with NiO nanoparticles, *J. Non. Cryst. Solids*. 522, (2019)  
<https://doi.org/10.1016/j.jnoncrysol.2019.119566>
- [8] R. J. Amjad, M.R, Dousti, M. R. Sahar, S.F. Shaukat, S.K. Ghoshal, E.S. Sazali, F. Nawaz. Silver nanoparticles enhanced luminescence of Eu<sup>3+</sup>-doped tellurite glass, *J. Lumin.* 154, 316-321, (2014)  
<https://doi.org/10.1016/j.jlumin.2014.05.009>
- [9] M. Abbas. Structural, Thermal, Optical and Dielectric Studies On Rare Earth Ion-Doped Borate Glasses for Solid State Laser Application, PhD dissertation, Universiti Putra Malaysia, Serdang, Malaysia (2019)
- [10] Y. Azlina, M.N. Azlan, M.K. Halimah, S.A. Umar, G. Najmi. Optical performance of neodymium nanoparticles doped tellurite glasses *Phys. B Condens. Matter*. 577, 411784 (2020)  
<https://doi.org/10.1016/j.physb.2019.411784>
- [11] H. R. Shaari, M.N. Azlan, Y. Azlina, S.S. Hajer, S.N. Nazrin, S.A. Umar, B.K. Kenzhaliyev, I. Boukhris, N.M. Al-Hada, N. M. Investigation of Structural and Optical Properties of Graphene Oxide Coated Neodymium Nanoparticles Doped Zinc Tellurite Glass for Glass Fiber, *J. Inorg. Organomet. Polym. Mater.* 31, 4349-4359 (2021)  
<https://doi.org/10.1007/s10904-021-02061-7>
- [12] Y. Azlina, M. N. Azlan, A. B. Suriani, M. K. Halimah, and S. A. Umar. Optical properties of graphene oxide-coated tellurite glass for potential fiber optics, *J. Non. Cryst. Solids*. 536, 120000 (2020)  
<https://doi.org/10.1016/j.jnoncrysol.2020.120000>
- [13] N. Md Disa. Synthesis Of Graphene Oxide Using Electrochemical Exfoliation Method For Electrode Materials Application, Phd dissertation, Universiti Pendidikan Sultan Idris, Tanjong Malim, Malaysia (2017)
- [14] F. M. Fudzi, H. M. Kamari, F. D. Muhammad, A. A. Latif, and Z. Ismail. Structural and Optical Properties of Zinc Borotellurite Glass Co-Doped with Lanthanum and Silver Oxide, *J. Mater. Sci. Chem. Eng.* 6 (4), 18-23 (2018)  
<https://doi.org/10.4236/msce.2018.64003>

- [15] A. A. Awshah, M.K. Halimah, K.T. Chan, M.S. Nurisya, H.A. Salah, S.A. Umar, N.A.A. Muhammad. Effect of Neodymium Nanoparticles On Elastic Properties Of Zinc Tellurite Glass System, *Adv. Mater. Sci. Eng.* 2017, 1-7 (2017).
- [16] N. Md Disa, S. Abu Bakar, S. Alfarisa, A. Mohamed, I. Md Isa, A. Kamari, M. Rusop Mahmood. The Synthesis of Graphene Oxide via Electrochemical Exfoliation Method, *Adv. Mater. Res.* 1109, 55-59 (2015)  
<https://doi.org/10.4028/www.scientific.net/AMR.1109.55>
- [17] S. N. Kazi, A. Badarudin, M.N.M. Zubir, H.N. Ming, M. Misran, E. Sadeghinezhad, M. Mehrali, N.I. Syuhada. Investigation on the use of graphene oxide as novel surfactant to stabilize weakly charged graphene nanoplatelets, *Nanoscale Res. Lett.* 10(1), 16-18 (2015)  
<https://doi.org/10.1186/s11671-015-0882-7>
- [18] M. K. Halimah, S. N. Nazrin, and F. D. Muhammad, "Influence of silver oxide on structural, physical, elastic and optical properties of zinc tellurite glass system for optical application, *Chalcogenide Lett.* 16 (8), 365-385 (2019)
- [19] B. C. Jamalaiah. GeO<sub>2</sub> activated tellurite tungstate glass: A new candidate for solid state lasers and fiber devices, *J. Non. Cryst. Solids.* 502, 54-61(2018)  
<https://doi.org/10.1016/j.jnoncrysol.2018.03.032>
- [20] M. N. Azlan, M. K. Halimah, R. El-Mallawany, M. F. Faznny, and C. Eevon. Optical properties of zinc borotellurite glass system doped with erbium and erbium nanoparticles for photonic applications, *J. Mater. Sci. Mater. Electron.* 28, 4318-4327 (2017)  
<https://doi.org/10.1007/s10854-016-6056-2>
- [21] M. K. Halimah, A. A. A. Awshah, A. M. Hamza, K. T. Chan, S. A. Umar, S. H. Alazoumi. Effect of neodymium nanoparticles on optical properties of zinc tellurite glass system, *J. Mater. Sci. Mater. Electron.* 31(5), 3785-3794 (2020)  
<https://doi.org/10.1007/s10854-020-02907-9>
- [22] G. Neelima, K. V. Krishnaiah, N. Ravi, K. Suresh, K. Tyagarajan, T. J. Prasad. Investigation of optical and spectroscopic properties of neodymium doped oxyfluoro-titania-phosphate glasses for laser applications, *Scr. Mater.* 162, 246-250 (2019)  
<https://doi.org/10.1016/j.scriptamat.2018.11.018>
- [23] C. R. Kesavulu, K. Suresh, J. F. M. dos Santos, T. Catunda, H. J. Kim, C. K. Jayasankar. Spectroscopic investigations of 1.06  $\mu\text{m}$  emission and time resolved Z-scan studies in Nd<sup>3+</sup>-doped zinc tellurite based glasses, *J. Lumin.* 192, 1047-1055 (2017)  
<https://doi.org/10.1016/j.jlumin.2017.08.037>
- [24] M. N. Azlan , M.K. Halimah , S.S. Hajer, A.B. Suraini, Y. Azlina, Umar, S. A. Enhanced Optical Performance of Tellurite Glass Doped with Samarium Nanoparticles for Fiber Optics Application, *Chalcogenide Lett.* 16(5), 215-229 (2019)
- [25] B. Heidari, A. Majdabadi, L. Naji, M. Sasani Ghamsari, Z. Fakharan, and S. Salmani. Thin reduced graphene oxide film with enhanced optical nonlinearity, *Optik.* 156, 104-111 (2018)  
<https://doi.org/10.1016/j.ijleo.2017.10.176>
- [26] K. P. Loh, Q. Bao, G. Eda, and M. Chhowalla. Graphene oxide as a chemically tunable platform for optical applications, *Nat. Chem.* 2 (12), 1015-1024 (2010)  
<https://doi.org/10.1038/nchem.907>
- [27] M. K. Halimah, M. F. Faznny, M. N. Azlan, H. A. A. Sidek. Optical basicity and electronic polarizability of zinc borotellurite glass doped La<sup>3+</sup> ions, *Results Phys.* 7, 581-589 (2017)  
<https://doi.org/10.1016/j.rinp.2017.01.014>
- [28] V. Dimitrov and T. Komatsu. Electronic Ion Polarizability, Optical Basicity and Metal ( or Nonmetal ) Binding Energy of Simple Oxides, *J. Ceram. Soc. Japan.* 107 (10), 879-886 (1999)  
<https://doi.org/10.2109/jcersj.107.879>
- [29] V. Dimitrov and T. Komatsu. An Interpretation of Optical Properties of Oxides and Oxide Glasses in Terms of the Electronic Ion Polarizability and Average Single Bond Strength, *J. Univ. Chem. Technol. Metall.* 45 (3), 219-250 (2010)
- [30] A. S. Asyikin, M. K. Halimah, A. A. Latif, M. F. Faznny, and S. N. Nazrin. Physical, structural and optical properties of bio-silica borotellurite glass system doped with samarium oxide nanoparticles. *J. Non. Cryst. Solids.* 529, 119777 (2020)  
<https://doi.org/10.1016/j.jnoncrysol.2019.119777>

- [31] S. A. Umar, M. K. Halimah, K. T. Chan, and A. A. Latif. Polarizability, optical basicity and electric susceptibility of Er<sup>3+</sup> doped silicate borotellurite glasses, *J. Non. Cryst. Solids.* 471, 101-109 (2017)  
<https://doi.org/10.1016/j.jnoncrysol.2017.05.018>
- [32] P. Gayathri Pavani, K. Sadhana, and V. Chandra Mouli. Optical, physical and structural studies of boro-zinc tellurite glasses, *Phys. B Condens. Matter.* 406 (6-7), 1242-1247 (2011)  
<https://doi.org/10.1016/j.physb.2011.01.006>
- [33] M.N. Azlan. Linear and non-linear optical properties of Zinc Borotellurite Glass Doped with Erbium, Erbium Nanoparticles, Neodymium and Neodymium Nanoparticles. PhD. dissertation, Universiti Putra Malaysia, Serdang, Malaysia (2016)  
<https://doi.org/10.1016/j.jlumin.2016.09.047>
- [34] V. Dimitrov and S. Sakka. Electronic oxide polarizability and optical basicity of simple oxides, *I. J. Appl. Phys.* 79 (3), 1736-1740 (1996)  
<https://doi.org/10.1063/1.360962>
- [35] V. Aruna, S. Yusub, M. Venkateswarlu, A. Ramesh Babu, and K. Anitha. Efficacy of copper ions on lithium ion conductivity, electron hopping, optical band gap, metallization criterion and morphology of Li<sub>2</sub>O-B<sub>2</sub>O<sub>3</sub>-P<sub>2</sub>O<sub>5</sub> glasses, *J. Non. Cryst. Solids.* 536, 120015 (2020)  
<https://doi.org/10.1016/j.jnoncrysol.2020.120015>
- [36] H. Algarni, M. Reben, and E. Yousef. Optical features of novel fluorotellurite glasses based on TeO<sub>2</sub>-LiNbO<sub>3</sub>-BaF<sub>2</sub>-La<sub>2</sub>O<sub>3</sub>-(Nb<sub>2</sub>O<sub>5</sub> or TiO<sub>2</sub>), *Optik.* 156, 720-727 (2018)  
<https://doi.org/10.1016/j.jleo.2017.12.001>
- [37] C. Devaraja, G. V. J. Gowda, B. Eraiah, and K. Keshavamurthy. Optical properties of bismuth tellurite glasses doped with holmium oxide, *Ceram. Int.* 47 (6), 7602-7607 (2021)  
<https://doi.org/10.1016/j.ceramint.2020.11.099>
- [38] A. A. Awshah. Physical, Structural, Elastic and Optical properties of Neodymium Oxide Doped Zinc Tellurite Glass System with Silver Incorporation. PhD dissertation. Universiti Putra Malaysia, Serdang, Malaysia (2019)